Comment on "Activation Rate of Seismicity for Hydraulic Fracture Wells in the Western Canadian Sedimentary Basin" by Hadi Ghofrani and Gail M. Atkinson

James P. Verdon*[1] and Julian J. Bommer[2]

KEY POINTS

- We address the Ghofrani and Atkinson (2020) claims that seismicity is linked to stimulation of shallow reservoirs.
- Detailed reanalysis of their cases shows the claimed links are spurious.
- There are no cases of stimulation-induced seismicity from shallow formations in the WCSB.

It is well established that injection of fluids into the subsurface can cause induced seismicity. Cases of injection-induced seismicity have been documented during wastewater disposal, hydraulic fracturing (HF), and geothermal energy production. However, attribution of seismic activity to specific causative activities can be challenging (e.g., Verdon, Baptie, and Bommer, 2019). It is important to correctly ascertain when and where seismic events have been induced by human activities. In cases in which multiple activities take place in the subsurface, it is equally important to ascertain which activities have been responsible for causing induced seismicity.

The correct attribution of induced seismicity has importance both for the appropriate regulation of subsurface industries, and for our scientific understanding of this phenomenon. Establishment of causation has great significance when establishing the seismic risk posed by different types of subsurface activity (and by the same type of activity conducted in different formations or geological settings). Probabilistic assessments of seismic risk are typically driven by extrapolation from past observations of seismicity. Hence, accurate characterizations of observed rates and magnitudes of induced seismicity are required. This issue has enormous implications for livelihoods and for public safety. If seismic events are incorrectly thought to have been induced by a particular activity, when they are in fact natural (or induced by a different activity), then regulators may respond with increased regulatory burdens, or even outright bans, creating a significant impact to the livelihoods of those working in the industry in question, as well as impacting the wider economic benefits that an industry might provide to a particular area. On the other hand, if seismic events are incorrectly characterized as natural when they have in fact been induced, then appropriate mitigation may not be applied in which it is necessary, resulting in an increased level of seismic risk that could otherwise have been avoided.

From a scientific perspective, we are increasingly seeing studies that use compilations of induced seismicity cases to learn more about the key factors and processes that govern induced seismicity (e.g., Eaton and Igonin, 2018; Foulger *et al.*, 2018; Pawley *et al.*, 2018; Baisch *et al.*, 2019; Verdon and Bommer, 2021). If cases are included in such compilations that are not actually induced, or in which the causative activity is incorrectly ascribed, then the learnings that we might otherwise make from such compilations may not be valid.

We are writing this comment to address the estimates made by Ghofrani and Atkinson (2020, hereafter, GA20) of recurrence rates (i.e., number of cases per stimulated well) of hydraulic fracturing-induced seismicity (HF-IS) as a function of different formations in the western Canadian sedimentary basin (WCSB), with a particular focus on their claims that HF-IS has been caused by operations in shallower formations within the basin, such as the Cretaceous Mannville, Cardium, and Dunvegan.

In the WCSB, HF-IS has been clearly demonstrated from stimulation of the Upper Devonian Horn River (disaggregated by GA20 into the Muskwa, Evie, and Otter Park members) (Farahbod *et al.*, 2015), the Upper Devonian Duvernay (e.g., Bao and Eaton, 2016), and Lower Triassic Montney (e.g., Roth *et al.*, 2020) shale formations.

Cases of induced seismicity in the WCSB have also been identified from wastewater disposal operations in deep formations (e.g., Schultz *et al.*, 2014; Anderson and Eaton, 2016;

1. School of Earth Sciences, University of Bristol, Bristol, United Kingdom, https://orcid.org/0000-0002-8410-2703 (JPV); 2. Department of Civil and Environmental Engineering, Imperial College London, London, United Kingdom, https://orcid.org/0000-0002-9709-5223 (JJB)

*Corresponding author: james.verdon@bristol.ac.uk

Cite this article as Verdon, J. P., and J. J. Bommer (2021). Comment on "Activation Rate of Seismicity for Hydraulic Fracture Wells in the Western Canadian Sedimentary Basin" by Hadi Ghofrani and Gail M. Atkinson, *Bull. Seismol. Soc. Am.* **XX**, 1–16, doi: 10.1785/0120200350

Hosseini and Eaton, 2018), and from conventional hydrocarbon operations (e.g., Wetmiller, 1986; Baranova *et al.*, 1999), although it is by no means clear whether the seismicity at Rocky Mountain House is in fact generated by conventional production or by collocated wastewater injection into underlying formations.

The cases of induced seismicity in the earlier-referenced studies were all caused by hydrocarbon operations in Palaeozoic or lower Mesozoic formations. GA20 is the first study that we are aware of that has presented a claim for HF-IS in the WCSB having been caused by operations targeting shallower formations situated above the lower-Cretaceous unconformity. This major, basinwide unconformity separates carbonate-dominated Palaeozoic (and lower Mesozoic) sediments, deposited on a passive extensional or transtensional margin, from the clastic-dominated Cretaceous and Cenozoic sediments deposited in a foreland basin created by uplift of the sierras to the west and south (Mossop and Shetsen, 1994). The shallower formations being targeted in the Cretaceous section are, broadly speaking, tight sandstone plays rather than shale formations. It is not disputed that HF and wastewater disposal in Palaeozoic formations has generated induced seismicity with magnitudes $\mathbf{M} > 3$. However, GA20 claim that the rates of seismicity generated by HF in the Dunvegan and Gething formations (association percentage of 0.7% at $W > 0.35$, table 2 of GA20) are of a similar order of magnitude to the rate at which the Montney formation has generated induced seismicity (association percentage of 1.5% at $W > 0.35$), and that seismicity has also been generated by stimulation of the Cardium and Mannville formations.

The method used by GA20 uses extremely loose spatiotemporal criteria to assign induced seismicity associations, and it fails to consider the impacts of the overlap that exists between different types of operation within the WCSB. As a result, the links made by GA20 between seismicity and hydraulic stimulation of shallower formations in the WCSB are erroneous.

THE GHOFRANI AND ATKINSON (2020) METHOD

There is a growing body of literature that describes how seismicity can be assessed as being natural or induced, and if induced, by which activity (e.g., Davis and Frohlich, 1993; Davis *et al.*, 1995; Cesca *et al.*, 2012; Dahm *et al.*, 2013, 2015; Passarelli *et al.*, 2013; Oprsal and Eisner, 2014; Goebel *et al.*, 2015; Schoenball *et al.*, 2015; Frohlich *et al.*, 2016; Verdon, Baptie, and Bommer, 2019). The waveforms generated by induced earthquakes are not significantly different from those generated by natural earthquakes. As such, causation is usually established via considerations of temporal correlation between seismicity and the activity in question, spatial proximity (both laterally and, where earthquake depths are constrained, in depth), precedent and past rates of activity (both of natural seismicity rates and of seismicity generated by similar industrial activities), and considerations of whether the activity in question could have created a hydraulic or geomechanical perturbation at the earthquake hypocenter of sufficient size and mechanism to have triggered the event.

It is notable that GA20 do not engage with any of the approaches proposed in these studies. The GA20 method is based solely on spatiotemporal coincidence, in which values are assigned to a parameter, W, on the basis of separation between the HF well pad and earthquake epicenter (taking a value of 1 for distances ≤3 km) and of time after the start of the HF (taking a value of 1 for intervals of five days or less); the final value of W, which indicates the likelihood of association, is the average of the two values determined from the windows of distance and time. A value of $W = 0.35$, the level described by GA20 "as passing a reasonable threshold for association" could be obtained, for example, by an earthquake occurring at 20 km from a hydraulically fractured well within 10 days of stimulation or by an earthquake occurring at 4.5 km from a well within 90 days of stimulation. A value of $W = 0.5$ (the highest level in table 2 of GA20) could be obtained by an event that is 20 km from a well within 5.7 days of stimulation, or at 3.3 km from a well within 90 days of stimulation. A striking aspect of the nature of GA20's method of calculating W via an arithmetic mean of the spatial and temporal weightings is that a value of $W = 0.5$ can be obtained even when one of the weighting factors (W_T or W_D) is equal to zero. In other words, an association between the earthquake and a specific well can be inferred despite being scored as impossible in terms of either space or time.

We also note in passing that although GA20 describe $W \geq 0.35$ as "a reasonable threshold for association," they later argue that results from $W \geq 0.25$ are statistically significant. In their table 2, GA20 include association rates from W-values down to $W \geq 0.15$, and events with $W \geq 0.15$ are included in their table A1 of associated events, producing a potential ambiguity for the reader with respect to an appropriate W-value for potential association.

Irregardless of the choice of W threshold, the criteria for spatiotemporal coincidence used by GA20 are remarkably loose. Verdon and Bommer (2021) investigated the temporal evolution of HF-IS from case studies around the world. If an induced event were to occur after the end of stimulation, when no seismicity had been recorded during operations, a postinjection increase in magnitude would have occurred. The largest time lag observed between the end of HF and an increase in seismic magnitudes was 23 days (Verdon and Bommer, 2021). Hence, the 90-day window allowed by GA20 (a time lag with which an event could still score a W-value as high as 0.5) is almost four times larger than the longest lag ever observed for a case of HF-IS.

Similarly, where high-resolution local monitoring networks have been used to monitor HF-IS, events locations are found to be at most within 1–2 km of the causative well (e.g., Bao and Eaton, 2016; Eaton *et al.*, 2018; Clarke *et al.*, 2019; Kettlety *et al.*,

2019; Kettley, Verdon, Hampson, and Craddock, 2020; Kettley, Verdon, Werner, and Kendall, 2020). GA20 argue for the larger distances allowed by their *W* parameter based on event location uncertainties and the use of horizontal drilling. However, the publicly available database of stimulated wells provided by the Alberta Energy Regulator includes both surface and well-bottom coordinates, so it is possible to explicitly include deviated wells in any assessment of spatiotemporal coincidence.

GA20 claim that the typical location uncertainty of catalog events in the WCSB is approximately 10 km. Their estimate is based on discrepancies in epicentral locations quoted by different monitoring agencies. This is not an appropriate way to determine location uncertainties where different networks are used to locate the same event. A discrepancy in event location might be expected if one agency (such as the Alberta Geological Survey [AGS]) was using a denser, regional network, whereas another (e.g., the Canadian National Seismograph Network) was using a more sparse, national monitoring network. Any location discrepancies would reflect the larger uncertainties in the lower-resolution network, and they would not define the precision of the denser-resolution network. Schultz *et al.* (2015) performed an assessment of the AGS seismic network capability and found location uncertainties typically ranging from <1 to 3 km for $\mathbf{M} \geq 3.0$ events across much of the area of interest where oilfield activities are taking place in Alberta.

Given that location uncertainties are expected to be within 3 km, and that events are generally found to occur within 2 km of a causative well when high-quality local monitoring is available, a maximum distance of 5 km from any part of the subsurface well track might be a more suitable cutoff.

A more significant shortcoming of the GA20 approach is that no other potential anthropogenic causes were considered. As described earlier, it is well established that induced seismicity in the WCSB has been caused by HF in the Duvernay, Montney, and Horn River shale formations, and by wastewater disposal in certain formations. When associating induced seismicity with other activities, such as HF in shallower formations, the dominant seismicity signal from the known seismogenic activities must first be accounted for. Otherwise, the GA20 method could still associate an event with a relatively weak *W* score with a given well, when in fact there is a far more clear and obvious cause. In fact, the most obvious utility of the GA20 approach would be to use relative *W* scores for different subsurface activities around the same earthquake to establish the most likely cause of an event.

GA20 use a Monte Carlo simulation to assess the statistical significance of their results. A Monte Carlo simulation would be a valid way of assessing statistical significance if the null hypothesis was that earthquakes were occurring randomly. This would be a reasonable assumption for a comparison with natural earthquake genesis. However, it is well established that HF in the Horn River, Montney, and Duvernay shales, and wastewater disposal in deeper formations, has driven much of the seismicity observed in the WCSB over the last few decades. As a result, the occurrence of seismicity is not random, but will occur in spatial and temporal correlation with these activities, and so random earthquake genesis is not an appropriate null hypothesis when assessing whether HF in shallower formations has also caused induced seismicity. HF wells in shallower formations will have a much higher chance of being linked to earthquakes using the GA20 method in which they are found in proximity to the deeper Duvernay, Montney, or Horn River wells, or seismogenic waste disposal wells, but this association will be coincidental.

Thus, GA20 have used a Monte Carlo simulation to examine the ability of the *W* parameter to discriminate between induced and natural events. However, they have not tested its ability to discriminate between different potential causes of induced seismicity, which is the key conclusion of the GA20 study, over and above the findings of Atkinson *et al.* (2016). As such, their conclusions regarding rates at which induced seismicity has been triggered in different formations in the WCSB are not supported by the modeling that they have presented. Consequently, these association rates cannot be used to characterize how often shallower wells generate induced seismicity (or indeed whether they generate any induced seismicity at all).

REASSESSMENT OF GHOFRANI AND ATKINSON (2020) CASES

GA20 argue that their model is probabilistic, and that although some false positives will be generated by their loose spatiotemporal criteria, their use of summed *W*-values will account for the false positives. The validity of their approach is based on a top-down assessment of the association rates that are produced—they are similar to previous rates found by Atkinson *et al.* (2016). We note that Atkinson *et al.* (2016) used similar criteria in their assessment, and the fact that similar methods produce similar results is a circular argument and not a validation (in and of itself) of the method.

More importantly, a bottom-up assessment of the credibility of their method is also possible. There remains a deterministic element to the GA20 approach, because their results present a description of what has happened; they are not a forecast of what might happen going forward. Their approach associates specific earthquakes with specific HF wells to calculate rates of induced earthquakes above a certain magnitude per well, and as such it is possible to examine each case in detail to investigate whether the potential association is credible.

For wells targeting Cretaceous formations (Cardium, Dunvegan, Gething, Cadomin, Glauconitic Sandstone, Basal Belly River Sandstone, as per GA20 table 2), GA20 identify only 11 wells at the $W \geq 0.35$ level. This is a very small population of cases with which to make any probabilistic assessment of results. When performing any top-down assessment of the statistical

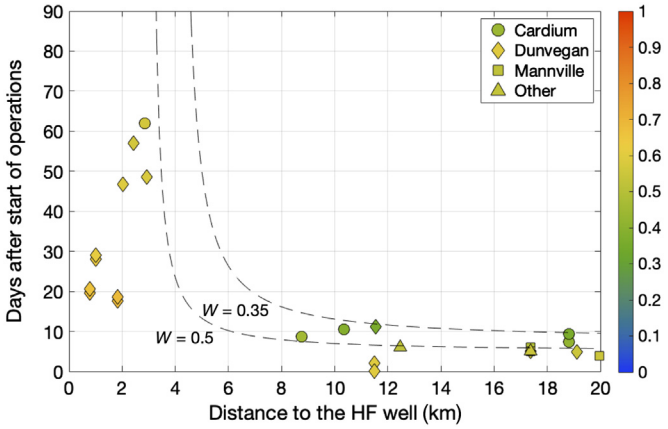

Figure 1. *W*-values for all earthquakes with $W \geq 0.35$ for wells targeting Cretaceous strata, showing the distance between each well pad and event, and the time lag between the event and the start of operations. Symbol shapes represent different formations and are colored by the *W* score. The color version of this figure is available only in the electronic edition.

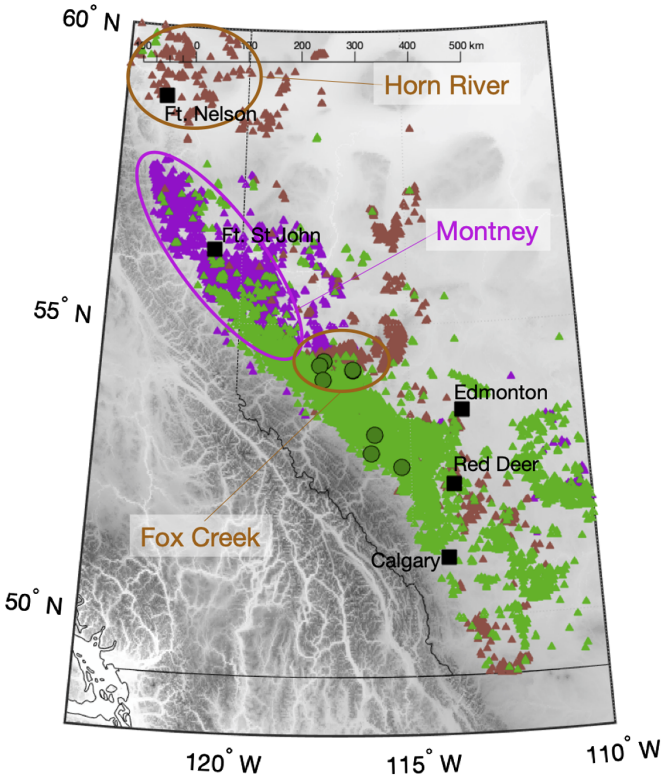

Figure 2. Map showing locations of earthquakes (green dots) from 2009 onward, with **M** ≥ 3, that are linked by the Ghofrani and Atkinson (2020, hereafter, GA20) method to wells stimulating Cretaceous strata (with $W \geq 0.35$). We also show all wells stimulated in Devonian (brown triangles), Triassic (purple triangles), and Cretaceous (green) formations. Three areas where cases of hydraulic fracturing-induced seismicity (HF-IS) have been prominent are marked: Horn River, where seismicity has been caused by operations in the Horn River Shale; the Montney trend; and Fox Creek, where seismicity has been caused by operations in the Duvernay formation. The color version of this figure is available only in the electronic edition.

results, this small number of cases will be lost among the hundreds of cases of induced seismicity generated by the Montney and Duvernay formations (which we agree have generated HF-IS at high rates).

For the small number of cases in Cretaceous formations, it is far more appropriate to perform a bottom-up assessment, in which the validity of each individual event and well can be examined on a case-by-case basis to evaluate whether the association proposed by GA20 is credible. In the following section (and continued in the Appendix), we adopt this approach, examining in detail every single case in which an association with $W \geq 0.35$ between an **M** ≥ 3.0 event and a hydraulically fractured well targeting Cretaceous formations could be found.

GA20 did not specify which events they linked to which specific wells targeting Cretaceous formations. This critical information, specifying which **M** ≥ 3.0 events are linked to which specific wells that make up the Cretaceous formation cases in GA20 table 2 has not been provided. Therefore, to assess events on a case-by-case basis, we have repeated GA20's analysis. Following GA20, we used **M** ≥ 3.0 earthquakes listed in the Composite Alberta Seismicity Catalog from 2009 to April 2019, and the well database provided by the Alberta Energy Regulator. Table 1 lists all earthquakes that we have identified as having $W \geq 0.35$ when paired with a well targeting a formation of Cretaceous. In total, we identified 25 $W \geq 0.35$ pairs, corresponding to nine unique earthquakes, and 17 unique wells. We plot the distribution of well-event distances and time lags in Figure 1, and a map of identified events in Figure 2 (in these figures and tables we refer to all wells targeting members of Mannville [Aptian to early Albian], including the Fahler; Ostracod Beds; Cadomin; Glauconitic Sand; Bluesky; Gething; Spirit River; Wilrich; Notikewin; Ellerslie, as "Mannville"). Because GA20 did not specify which earthquakes they have associated with which wells, it is not possible to confirm that the cases in Table 1 correspond exactly to the cases identified by GA20, but we have identified similar numbers of events within the different Cretaceous formations as GA20 (as per their table 2), with similar distributions of *W*-values, indicating that we have very likely identified the same cases.

In the following, we examine these cases in more detail, highlighting how they demonstrate the flaws in the GA20 approach that we described above. In the Appendix, we provide a commentary for every case listed in Table 1, which likely represent the entire population of events that have been "associated" by the GA20 method with HF of Cretaceous formations in the WCSB. GA20 accept that their method will produce some false positives. Therefore, the fact that we have examined every single case in which **M** ≥ 3.0 seismicity has been supposedly linked to HF of Cretaceous wells, as identified by the GA20 method, is of significance, because we find that all of

TABLE 1
Listing of All Events and Associated Cretaceous Wells with $W \geq 0.35$

Event Date/Time (yyyy/mm/dd hh:mm:ss)	Magnitude	Latitude (°)	Longitude (°)	Unique Well Identifier (UWI) and Formation	*W*	Well–Event Distance (km)	Lag (Days)
2009/08/10 02:38:46	3.0	54.07	−117.49	100/07-18-057-23W5/03 Mannville	0.49	17.4	6
⋮	⋮	⋮	⋮	100/07-18-057-23W5/02 Mannville	0.49	17.4	6
⋮	⋮	⋮	⋮	100/07-18-057-23W5/04 Mannville	0.55	17.4	5
⋮	⋮	⋮	⋮	100/07-18-057-23W5/05 Dunvegan	0.55	17.4	5
⋮	⋮	⋮	⋮	100/07-18-057-23W5/06 Colorado	0.55	17.4	5
2010/10/08 20:14:24	3.2	53.12	−116.02	100/13-13-050-15W5/00 Mannville	0.55	20.0	4
2013/01/01 01:01:00	3.0	52.81	−116.11	102/10-09-044-15W5/00 Cardium	0.57	2.9	62
2015/01/15 19:18:29	3.3	54.38	−117.46	100/05-13-062-26W5/00 Dunvegan	0.55	19.1	5
2017/01/16 02:22:36	3.0	54.31	−117.59	100/04-13-062-26W5/00 Dunvegan	0.36	11.54	11
2017/12/05 16:01:22	3.1	54.23	−116.63	100/12-18-060-17W5/00 Cardium	0.46	8.8	8
⋮	⋮	⋮	⋮	100/05-05-061-18W5/00 Dunvegan	0.68	1.8	18
⋮	⋮	⋮	⋮	100/13-32-060-18W5/00 Dunvegan	0.68	1.8	19
⋮	⋮	⋮	⋮	102/03-26-060-18W5/00 Dunvegan	0.59	2.0	47
2017/12/07 13:28:29	3.1	54.24	−116.64	100/12-18-060-17W5/00 Cardium	0.39	10.4	11
⋮	⋮	⋮	⋮	100/05-05-061-18W5/00 Dunvegan	0.67	0.8	20
⋮	⋮	⋮	⋮	100/13-32-060-18W5/00 Dunvegan	0.66	0.8	21
⋮	⋮	⋮	⋮	102/03-26-060-18W5/00 Dunvegan	0.58	2.9	49
2017/12/16 01:13:36	3.4	54.24	−116.64	100/05-05-061-18W5/00 Dunvegan	0.63	1.0	28
⋮	⋮	⋮	⋮	100/13-32-060-18W5/00 Dunvegan	0.62	1.0	29
⋮	⋮	⋮	⋮	102/03-26-060-18W5/00 Dunvegan	0.57	2.4	57
⋮	⋮	⋮	⋮	100/04-08-060-17W5/00 Dunvegan	0.60	11.5	2
⋮	⋮	⋮	⋮	100/05-08-060-17W5/00 Dunvegan	0.60	11.5	1
⋮	⋮	⋮	⋮	100/03-10-060-17W5/03 Viking	0.52	12.5	6
2019/03/10 10:00:36	3.8	52.57	−115.26	104/12-35-042-08W5/00 Cardium	0.42	18.8	7
⋮	⋮	⋮	⋮	102/13-35-042-08W5/02 Cardium	0.36	18.8	9

the identified cases are clearly false positives, and as such there are no cases in which HF of Cretaceous formations can be credibly linked to induced earthquakes with $\mathbf{M} \geq 3.0$.

Fox Creek Duvernay: 5 December 2017 M 3.1; 7 December 2017 M 3.1; 16 December 2017 M 3.4

This cluster of three $\mathbf{M} \geq 3.0$ earthquakes in the Fox Creek region, which occurred over a period of 11 days, was linked by the GA20 method to HF in one Cardium well (100/12-18-060-17W5/00), five Dunvegan wells (100/05-05-061-18W5/00; 100/13-32-060-18W5/00; 102/03-26-060-18W5/00; 100/04-08-060-17W5/00; 100/05-08-060-17W5/00), and one Viking well (100/03-10-060-17W5/03). However, in the Fox Creek area, induced seismicity has been extensively linked to HF of the Duvernay formation (e.g., Bao and Eaton, 2016).

Figure 3 shows a map of these events and their relationship to nearby wells. We observe that the events are collocated with a pad of four HF wells (102/06-28-060-18W5/00 100/05-28-060-18W5/00; 100/04-09-061-18W5/00; 102/03-09-061-18W5/00), all of which targeted the Duvernay formation. Each of these wells injected roughly 40, 000 m^3 of fluid from late November 2017 to early January 2018, and so stimulation in the Duvernay was active and ongoing when the events occurred. Two other events with $\mathbf{M}$ <3 were also collocated with these wells while stimulation was ongoing. The largest *W*-value calculated by GA20 for these events for the Duvernay wells is 0.81. However because HF in these wells took place over several weeks, stimulation was ongoing in the Duvernay wells when the events occurred, and so a *W*-value of 1.0 would be appropriate.

The events are more than 5 km from the nearest point of the Cardium well (100/12-18-060-17W5/00) track. This well only injected 3000 m^3, and stimulation finished on 28 November, seven days before the first event in the sequence began. The *W*-values for each of the three events when linked to this well are 0.39, 0.29, and 0.42. The events are more than 10 km from the Viking well, which only injected approximately 100 m^3, on 10 December, after the sequence of events had initiated.

Three of the Dunvegan wells (100/05-05-061-18W5/00, 100/13-32-060-18W5/00, and 102/03-26-060-18W5/00) are relatively close to the event sequence. Each of these wells injected approximately 3000 m^3 of fluid, with stimulation lasting only one day per well, conducted for the different wells on 20 October 2017, 18 November 2017, and 19 November 2017 (57, 29, and 28 days before the largest event on 16 December 2017). As discussed previously, a time lag of four weeks or more between the end of HF and an increase in event magnitudes would represent a longer lag than has ever

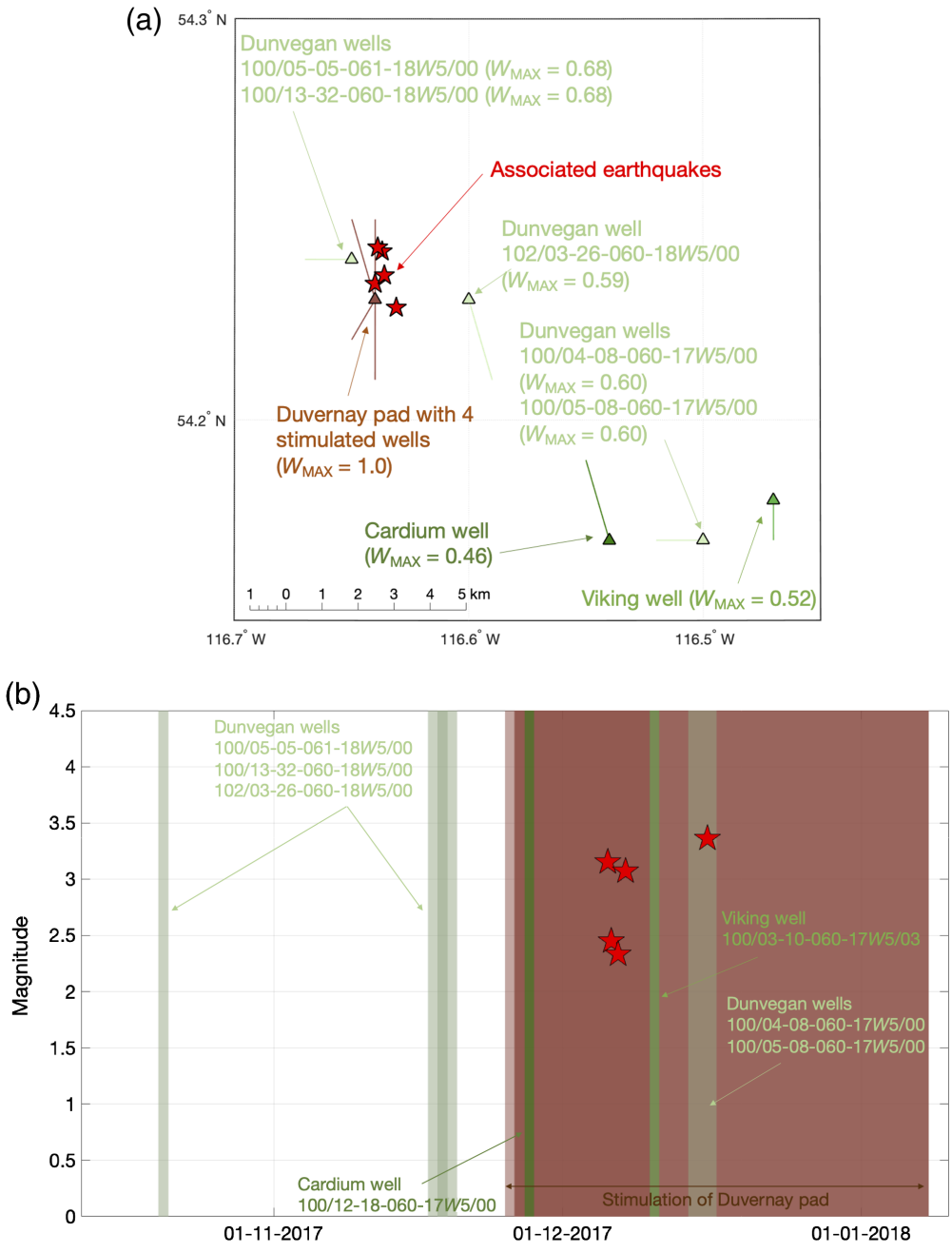

Figure 3. (a) Map and (b) timeline showing the three events occurring during December 2017 that were associated by the GA20 method with hydraulic fracturing (HF) in Cardium, Dunvegan, and Viking wells. The location of the Cardium well is shown by the dark green triangle (and lines showing the well track in the subsurface), and the locations of the Dunvegan wells by light green triangles and lines. Four Duvernay wells were also active at this time, shown by the brown diamond and lines. Five **M** ≥ 2.0 earthquakes that occurred during the time of interest are shown as red stars. Maximum *W*-values for each well (W_{MAX}) are also shown. In (b), we show the days in which HF took place in the Cardium (dark green), Dunvegan (light green), Viking (mid-green), and Duvernay (brown) wells, and the occurrence dates of the associated earthquakes. The color version of this figure is available only in the electronic edition.

been observed in any case study, suggesting that these wells acting as a cause for these events is extremely unlikely.

Two of the Dunvegan wells (100/04-08-060-17W5/00 and 100/05-08-060-17W5/00) were stimulated on 14 and 16 December, injecting approximately 3000 and 5000 m^3. Hence, these wells had not been stimulated at the time that the sequence of events began. The nearest point of these wells is located over 8 km from the event locations.

The collocation of events with the Duvernay wells, the fact that these Duvernay wells each injected an order of magnitude more fluid than the Cardium and Dunvegan wells, and the fact that the events occurred during stimulation of the Duvernay wells, provides a strong argument that these events were induced by the Duvernay HF. This is reflected in the high *W* score for the Duvernay wells. However, these events also score $W > 0.35$ for the wells targeting the Cretaceous formations and so would have been included in the GA20 summation to determine the rates at which Cretaceous formations produce HF-IS.

The events occur weeks after stimulation of the Dunvegan 100/05-05-061-18W5/00, 100/13-32-060-18W5/00, and 102/03-26-060-18W5/00 wells, and are not collocated with the Cardium, Viking, or with the Dunvegan wells 100/04-08-060-17W5/00 and 100/05-08-060-17W5/00. Furthermore, these shallow wells injected an order-of-magnitude less fluid than the Duvernay wells. Hence, we conclude that any links between the events and these Cretaceous wells are extremely weak. It is abundantly clear that these events were induced by HF in the Duvernay and, therefore, would have been erroneously included in the summation used by GA20 to estimate activity rates in Cretaceous formations.

We note that the "*W*" values for the Dunvegan wells ranged between $0.55 < W < 0.7$. These high values for the Dunvegan wells, despite the clear and obvious lack of causation between

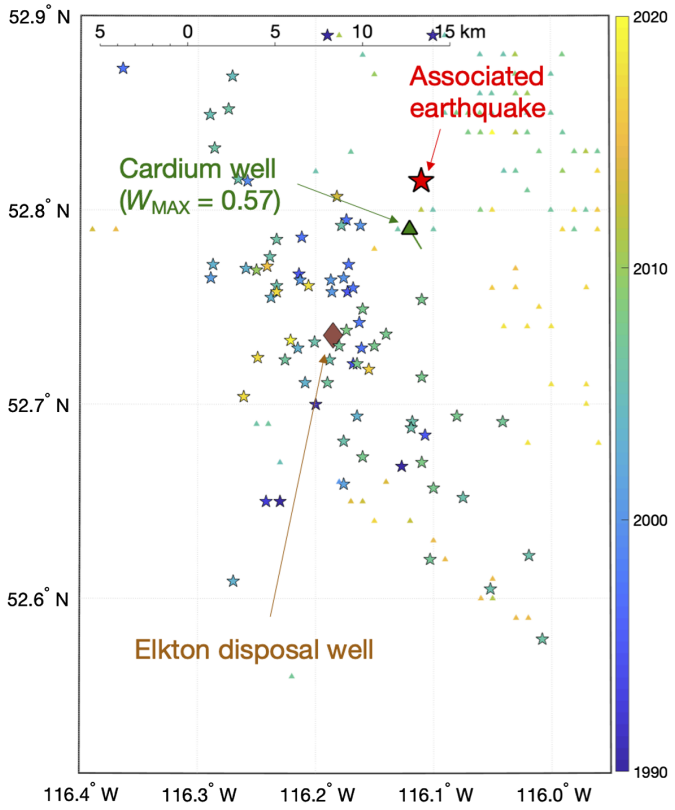

Figure 4. Map showing the event that occurred on 1 January 2013 in the Cordel cluster that was linked by the GA20 method with HF in a Cardium well (dark green triangle). A high-volume disposal well targeting the Elkton formation (Mississippian) is marked by a brown diamond. Other stimulated wells (triangles) are also shown, colored by the year in which stimulation took place. Stars show all **M** ≥ 2 earthquakes colored by their occurrence date—the event associated with the Cardium well is marked by a red star. The color version of this figure is available only in the electronic edition.

these wells and the events, demonstrates that even relatively high *W*-values cannot be taken as providing grounds for linking specific wells with specific earthquakes, unless further quality control assessments are undertaken.

We also note that the event epicenters are all located within 1–2 km of the Duvernay wells. The tight collocation between the events and the causative wells lends further evidence to the fact that location uncertainties for the most events in the catalog are relatively small, within the <1–3 km range estimated by Schultz *et al.* (2015) for the AGS earthquake catalog in this region.

Finally, the summed *W* scores for these events highlight a further flaw with the GA20 method. If one includes only Cretaceous wells, the summed *W* score for the largest of these events is 3.83. Although GA20 avoided double-counting wells in their assessment of association percentages (GA20, table 2), they appear to be double counting the same earthquake for multiple wells, such that one earthquake that occurred would be allowed to add up to almost four earthquakes in the association percentages.

Cordel: 1 January 2013 M 3.0

The GA20 method links a single earthquake within the Cordel cluster to a Cardium well (102/10-09-044-15W5/00), with $W = 0.57$. The seismicity in the Cordel cluster has been analyzed by Schultz *et al.* (2014), who concluded that these events were triggered by a high-volume water disposal well that is injecting into the Elkton formation (Mississippian).

Figure 4 shows a map of this event, and its relationship to adjacent oil and gas activities. Over 70 events with **M** ≥ 2 have been identified within the Cordel cluster. The onset of these events began in the early 1990s, after injection began in the 100/10-25-043-16W5/00 well and has continued to date. The event on 1 January 2013 is found within this cluster. The associated Cardium well is 3 km from the event. However, stimulation in this well ceased on 9 December 2012, 23 days before the event occurred. If this event was caused by the Cardium well it would match the longest ever delay observed between the end of a HF operation and an increase in induced event magnitude. More importantly, of the 13 **M** ≥ 3.0 events identified in the Cordel cluster, this is the only one that has any spatiotemporal match to any of the nearby HF wells. In contrast, Schultz *et al.* (2014) found that the correlation between injection rates in the 100/10-25-043-16W5/00 wastewater disposal well and the Cordel seismicity was statistically significant at a confidence level of 99%. It is not credible to claim that all other events in this cluster were driven by wastewater disposal, but that this single event was induced by HF. As such, the association identified by the GA20 method is not plausible.

Ferrier: 10 March 2019 M 3.8

This earthquake is the largest to have been linked by the GA20 method to HF of a well in Cretaceous strata. The GA20 method associates this event with two collocated Cardium wells (104/12-35-042-08W5/00 and 102/13-35-042-08W5/02). These wells both injected approximately 5000 m^3, from 1 March 2019 to 12 March 2019.

Figure 5 shows a map of this event and nearby oil and gas activities. As with the previous case, several hundred wells have been stimulated in Cretaceous strata within the area shown in Figure 5, and yet this is the only case where stimulation has been linked by the GA20 method to an **M** ≥ 3.0 earthquake.

The identified event is over 16 km from the linked wells. A location error far larger than 3 km (as estimated by Schultz *et al.*, 2015), and indeed larger than the 10 km location uncertainties adopted by GA20, would be required to collocate this event with these wells. This event has a magnitude of **M** 3.8, and occurs at a relatively central position within the AGS array, and so location uncertainties will be far smaller than this. The distance between this event and the identified wells means that any causative links are not plausible.

The event is located near to the Ferrier field, where a waterflood is being conducted for secondary recovery of conventional resources. Given the proximity of the location, this

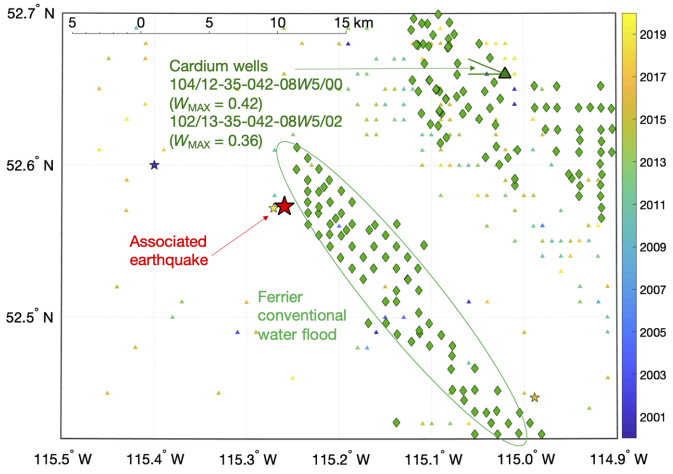

Figure 5. Map showing the event on 10 March 2019 (red star) that is linked by the GA20 method to two Cardium wells (green triangle, with lines marking the well track). The event is found near a swathe of injection wells (green diamonds) conducting a waterflood in the Ferrier field. Other earthquakes (stars) and HF wells (triangles) are shown, colored by their data of occurrence. The color version of this figure is available only in the electronic edition.

activity could be a more plausible cause for this event. However, the event hypocenter is located at 14 km depth. Given the event's larger magnitude, and its location within the AGS array, the depth uncertainties are relatively low; the depth uncertainty for this event in the AGS catalog is listed as being ±2 km. As such, the event depth is very likely to be more than 10 km and therefore too deep to have been caused by oilfield activities. An **M** 1.9 aftershock event that occurred later the same day had a similar location depth, indicating that this hypocentral location is robust. Whether or not the event has been caused by the waterflood in the Ferrier field, or is a natural event, it is certainly clear that this event has not been caused by HF in the Cardium wells over 15 km to the northeast, and that the link implied by the GA20 method is erroneous.

Summary of observations

In the Appendix, we provide similar commentaries for all the events listed in Table 1. In every case, a causative link between the identified events and the wells to which the GA20 method links them is not plausible or credible. Identified events can be clearly linked to HF of the Duvernay formation and to sequences of seismicity induced by wastewater disposal, and in some cases events are likely to have a natural origin. We conclude that the associations made by GA20 linking seismicity to HF in shallow, Cretaceous formations are all erroneous. When examining the cases identified using the GA20 method, we are unable to identify any cases in which **M** ≥ 3.0 earthquakes have been caused by HF of wells targeting Cretaceous strata in the WCSB, with over 10,000 such operations conducted over the past two decades.

DISCUSSION

The observations we have presented here merit further discussion with respect to the underlying structural geology and reservoir characteristics that may account for the different HF-IS response between the Duvernay, Horn River, and Montney shales, and shallower formations. Similar observations with respect to the very different levels of response between different formations at different depths in the same basin have been made in the Appalachian basin, where the shallower Marcellus Shale has not generated HF-IS, but cases have been recorded from the underlying Utica Shale (Skoumal *et al.*, 2018), and in the United Kingdom, where HF in the Bowland Shale has generated HF-IS (e.g., Clarke *et al.*, 2019; Kettlety, Verdon, Hampson, and Craddock, 2020), but stimulation in shallower conventional formations has not (Mustanen *et al.*, 2017).

We note that, for HF-IS to occur, pre-existing faults must be present that are well orientated in the in situ stress field, with the stress field having sufficient levels of shear stress (high stress anisotropy) such that faults are close to the Mohr–Coulomb failure surface (i.e., they are critically stressed). Furthermore, the HF must create a perturbation of sufficient size to be capable of reactivating a nearby fault. These criteria should inform explanations of why different formations have, or have not, generated induced seismicity.

Structural geology

As described in the introduction, the base of the Cretaceous represents a major, basinwide unconformity in the WCSB, with strata subcropping against this surface ranging in age from Devonian to Jurassic (Mossop and Shetsen, 1994). The Palaeozoic succession was deposited on an extensional or transtensional passive margin, with sediments sourced from the Canadian Shield to the northeast. The Cretaceous and Cenozoic succession was deposited in a foreland basin created by the uplift of sierras to the southwest, with sediments being sourced from that direction.

Given the different tectonic settings, it might be expected that few geological structures within the Palaeozoic would extend across the base-Cretaceous unconformity, and that there would be much greater potential for activities in the Palaeozoic rocks to impact basement-seated structures. This is found to be the case in practice. Ross and Eaton (1999) compared structures found in the basement to features in the overlying sedimentary sequences, and, in general, they did not find a strong relationship between the two. In the cases in which basement seated structures were observed extending into the overlying sediments, they were not found to extend any shallower than the lower Palaeozoic.

Similar observations have been made using a combination of reflection seismic imaging and microseismic monitoring from cases of HF-IS caused by stimulation of the Duvernay around Fox Creek (Eaton *et al.*, 2018; Eyre *et al.*, 2019). These observations have revealed fault reactivation on structures that have

grown from basement-seated transtensional faults that run through the Devonian section, terminating in the Wabamun formation (Famennian). Schultz and Wang (2020) have described similar observations during HF-IS cases around Red Deer, concluding that "hypocentre depths support a conceptual understanding of basement rooted faulting that extends just into the strata overlying the Duvernay Formation" (pp. 7–8).

These structural conditions may explain why HF in the Duvernay has generated cases of HF-IS with $\mathbf{M} \geq 3.0$ but stimulation of the overlying Cretaceous formations has not. We note that, even in the Fox Creek region, a significant number of wells have been stimulated in Cretaceous formations without generating any HF-IS. This shows that, even in a region that has experienced some of the highest levels of HF-induced seismicity in the entire WCSB, the fact that the basement-seated faults, which have been the cause of induced seismicity triggered by Duvernay stimulation, do not extend above the lower Cretaceous unconformity is likely to be a key factor in explaining why the shallower formations have not generated HF-IS.

The geological and structural setting in the region where the Montney formation has generated induced seismicity is substantially different to that around Fox Creek and Red Deer. Much of the HF-IS caused by stimulation of the Montney Shale has taken place within the fold-and-thrust best generated by the Laramide orogeny, and within the Peace River Arch. Within the Peace River Arch, the pre-Cambrian basement is significantly uplifted (Mossop and Shetsen, 1994), and there is a higher abundance of transtensional faulting extending from the basement. The compressional deformation associated with the Laramide orogeny has generated large north-northwest–south-southeast-trending thrust faults observable in reflection seismic datasets (e.g., Riazi *et al.*, 2020). These faults generally extend downward into Palaeozoic strata and upward into the Cretaceous section. It is on these thrust faults that induced seismicity in the Montney formation is observed to occur (e.g., Peña Castro *et al.*, 2020; Riazi *et al.*, 2020).

However, within the region where HF of the Montney has generated HF-IS, very little HF has taken place in Cretaceous strata (see Fig. 2). Some HF has taken place in the Cadomin (Early Cretaceous) formation in the Septimus-Dawson area to the southeast of Fort St. John. Injection volumes in these wells are typically insignificant (about 500 m^3 per well) relative to those used to stimulate the Montney formation (typically $>10,000$ m^3 per well), which represents the predominant activity in this area. $W \geq 0.35$ scores can be obtained for some events with magnitudes ranging from $2.0 < \mathbf{M} < 3.0$ and Cadomin wells in this area from July 2017. However, Roth *et al.* (2020) have analyzed this sequence in detail, using local seismometer networks to obtain an event catalog with high-precision event locations that is complete to approximately magnitude 1 and comparing this catalog with detailed injection records. Their results provide compelling evidence that the events are closely linked, in both space and time, to high-volume HF activities in the Montney formation, and any apparent links to low-volume Cadomin activities are clearly coincidental. Much like the cases we have discussed in the preceding section, this example showcases the pitfalls of relying solely on loose spatiotemporal criteria without examining in detail both the nature of different industrial activities and the full evolution of induced seismicity sequences.

Overall, however, the conditions that pertain to the Montney within the Laramide fold-and-thrust belt and Peace River Arch do not provide a good analog for the regions farther to the southeast where the majority of HF within Cretaceous formations has taken place.

Reservoir characteristics and operational parameters

The terms employed to characterize "unconventional" hydrocarbon development are often used loosely. HF is used to stimulate "shale" reservoirs, and it is also used to stimulate "tight sandstone" reservoirs, where the differentiation between these terms can be based both on the proportion of fine-grained clastic material, and also on the formation permeability.

The three formations that have generated HF-IS with $\mathbf{M} \geq 3.0$ in the WCSB can be considered to be shale formations, with typical permeabilities lying in the 1×10^{-7}–1×10^{-4} mD range (e.g., Chalmers, Bustin, and Bustin, 2012; Chalmers, Ross, and Bustin, 2012; Yassin *et al.*, 2017; Cui and Nassichuk, 2018; Ghanizadeh *et al.*, 2018). In contrast, most of the key unconventional reservoirs in the Cretaceous section, such as the Cardium, Mannville, and Dunvegan, would be better characterized as tight sandstones, with permeabilities lying in the 0.01–100 mD range (e.g., Arndt, 2017; Friesen *et al.*, 2017; Ghanbari *et al.*, 2019).

The higher permeabilities of these formations may have a direct impact on the nature of the perturbation caused by HF. Intuitively, it might be expected that a higher permeability might allow for hydraulic perturbations to travel farther. However, Verdon, Igonin, *et al.* (2019) showed how, for HF-IS in the Duvernay formation, the presence of pre-existing fracture corridors provided permeable pathways for fluid pressures to be transferred across a distance of approximately 1 km to reactivate a fault. In the case described by Verdon, Igonin, *et al.* (2019), pressures could be transferred over such distances, because the rock matrix permeability outside of the fracture corridor was low. If the rock matrix permeability (and porosity) were higher, elevated pressures created by the HF would be able to quickly dissipate into the matrix pore space, reducing the extent of the perturbation, and therefore reducing the likelihood of fault activation.

The reservoir permeability also determines the scale of HF operation needed to generate commercial hydrocarbon production rates. Very low permeability shale plays require high-volume stimulation, whereas the volumes used to

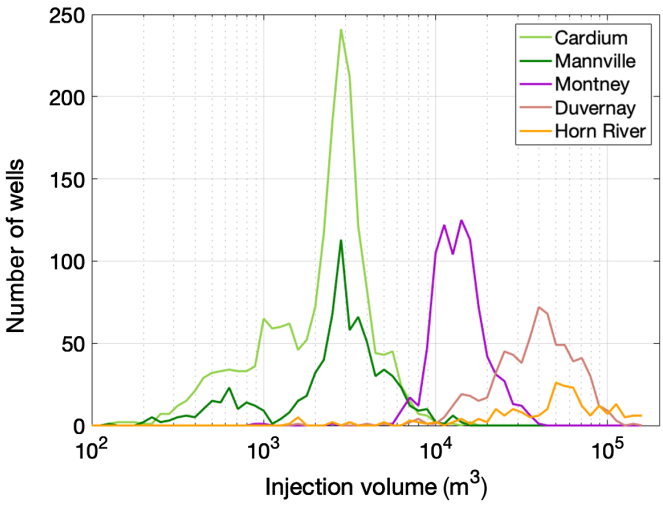

Figure 6. Injection volumes used per well for HF in different formations in the western Canadian sedimentary basin (WCSB). The color version of this figure is available only in the electronic edition.

stimulate tight sandstone reservoirs are smaller. Figure 6 shows the injection volumes used per well to stimulate the Cardium, Mannville, Dunvegan, Montney, Duvernay, and Horn River formations. For the shale formations, the mean per-well stimulation volumes are 54, 000 m^3 for the Horn River, 42, 000 m^3 for the Duvernay, and 14, 000 m^3 for the Montney. In contrast, for the Cretaceous tight sandstone formations, the mean per-well stimulation volumes are 3100 m^3 for the Mannville, 2500 m^3 for the Cardium, and 1900 m^3 for the Dunvegan. It is well established that rates and magnitudes of induced seismicity scale with injection volume (e.g., Shapiro *et al.*, 2010; McGarr, 2014; van der Elst *et al.*, 2016; Schultz *et al.*, 2018; Verdon and Budge, 2018), and so it is possible that the lower volumes used for HF in the shallower tight sandstone formations in the WCSB accounts for the absence of $\mathbf{M} \geq 3.0$ HF-IS observed for these formations.

It is beyond the scope of this comment to definitively establish why the Cretaceous tight gas formations in the WCSB have not generated any induced seismicity with $\mathbf{M} \geq 3.0$, whereas the deeper shale gas formations have. As described earlier, there are several plausible explanations that include the structural geology of the WCSB, the reservoir characteristics of the different formations, and the nature of the operations that are carried out. In addition, we have not examined the different states of stress that are present in the different formations, because public data with which to fully constrain spatial variations in the in situ effective stress tensor are limited. However, this could be another fruitful avenue of investigation because stress conditions are likely to be higher in deeper formations. Eaton and Schultz (2018) have shown that the occurrence of HF-IS seismicity in the Montney and Duvernay correlates with regions that are significantly overpressured, and Kettley, Verdon, Hampson, and Craddock (2020) have directly shown how the in situ stress conditions can control the extent to which faults can be reactivated by HF.

At a more general level, it is worth noting that HF has been used to stimulate conventional and tight reservoirs for many decades, without producing any notable cases of induced seismicity. This led the U.S. National Research Council (2013) to conclude that HF "does not pose a high risk for inducing felt seismic events." All of the cases of HF-IS that have been observed, because the National Research Council (2013) assessment have been caused by stimulation of shale formations (see Verdon and Bommer, 2021, for a list of case studies). In contrast, we are not aware of any significant cases of HF-IS being generated by stimulation of tight-gas sandstones. Future research might be usefully directed to developing a better understanding of why stimulation of tight sandstones, versus stimulation of certain shale gas plays, has generated such different levels and rates of induced seismicity.

CONCLUSIONS

GA20 have performed an assessment of the rates of induced seismicity generated by stimulation of different formations in the WCSB. They have done so on the basis of remarkably loose spatiotemporal coincidence criteria. Moreover, because it is well established that seismicity has been caused by HF in the Horn River, Montney, and Duvernay formations, and by wastewater disposal, any attempt to link seismicity to other activities in addition to these established causes must first account for this dominant signal. GA20 use a Monte Carlo simulation to assess the statistical significance of their result. The null hypothesis in their approach is random earthquake occurrence. Whereas this may be a suitable way to discriminate between natural and induced seismicity, it is not suitable for discriminating between different causes of induced seismicity, because in such a scenario the occurrence of earthquakes is not random. Because many Duvernay and Montney wells have generated induced events, any well that targeted shallower Cretaceous formations where operations in the Duvernay or Montney (or wastewater disposal in deep formations) were also ongoing nearby would have a much higher than random chance of being temporally and spatially coincident with an earthquake. However, this would not indicate that the event and the shallower well were linked in any way, unless further, detailed analysis were to provide evidence of such a link.

We have reevaluated every single case identified by the GA20 method in which HF in shallower formations (above the lower Cretaceous unconformity) has been linked to an $\mathbf{M} \geq 3.0$ seismic event. In all the cases identified, we find that there is no plausible or credible evidence to link events with HF in Cretaceous strata. Our findings are consistent with the literature on HF-IS in the WCSB to date, in which no cases of induced seismicity generated by stimulation of Cretaceous strata have been described.

We have identified sound reasons to account for the different induced seismicity responses between deeper, seismogenic formations in the WCSB, and the shallower formations that have not generated any induced seismicity. These reasons include the different structural geological settings of the different formations, their different reservoir properties, and the different scales of HF operations typically deployed in them. If induced earthquakes are incorrectly ascribed to activities that did not in fact cause them, then we will limit our ability to correctly identify the different factors that promote or inhibit induced seismicity. Similarly, if we incorrectly ascribe induced events to activities that did not cause them, then our assessments of the seismic hazard associated with these activities will be exaggerated, potentially resulting in the implementation of regulations or mitigating actions that are inappropriate and not needed.

DATA AND RESOURCES

The earthquake database used for this study was taken from the Composite Seismicity Catalog for Alberta and British Colombia, available at www.inducedseismicity.ca (last accessed September 2020). The hydraulic fracturing and waste disposal well database used for this analysis comes from the Alberta Energy Regulator (AER) Geologic Data Centre.

DECLARATION OF COMPETING INTERESTS

Both authors have acted as independent consultants for a variety of organizations including hydrocarbon operating companies and governmental organizations on issues pertaining to induced seismicity. Both authors have been retained to provide seismic hazard assessments for companies who are currently applying for licenses to conduct hydraulic fracturing in shallow formations in the western Canadian sedimentary basin (WCSB).

ACKNOWLEDGMENTS

The authors would like to thank Editor-in-Chief Thomas Pratt, Associate Editor Cezar Trifu, and Delphine Fitzenz and two anonymous reviewers for their constructive comments, which helped improve the quality of this article.

REFERENCES

Anderson, Z., and D. Eaton (2016). Induced seismicity due to wastewater injection near Peace River, Alberta, *Geoconvention Conf.*, Calgary, Alberta, 7–11 March 2016.

Arndt, K. K. (2017). Reservoir characterization and prediction of the lower cretaceous glauconite member at Jenner-Suffield field, Alberta, Canada, *M.Sc. Thesis*, Baylor University.

Atkinson, G. M., D. W. Eaton, H. Ghofrani, D. Walker, B. Cheadle, R. Schultz, R. Shcherbakov, K. Tiampo, J. Gu, R. M. Harrington, *et al.* (2016). Hydraulic fracturing and seismicity in the Western Canadian sedimentary basin, *Seismol. Res. Lett.* **87,** 1–17.

Baisch, S., C. Koch, and A. Muntendam-Bos (2019). Traffic light systems: To what extent can induced seismicity be controlled, *Seismol. Res. Lett.* **90,** 1145–1154.

Bao, X., and D. W. Eaton (2016). Fault activation by hydraulic fracturing in western Canada, *Science* **354,** 1406–1409.

Baranova, V., A. Mustaqeem, and S. Bell (1999). A model for induced seismicity caused by hydrocarbon production in the Western Canada sedimentary basin, *Can. J. Earth Sci.* **36,** 47–64.

Cesca, S., A. Rohr, and T. Dahm (2012). Discrimination of induced seismicity by full moment tensor inversion and decomposition, *J. Seismol.* **17,** 147–163.

Chalmers, G. R. L., R. M. Bustin, and A. A. M. Bustin (2012). Geological controls on matrix permeability of the Doig-Montney hybrid shale-gas–tight-gas reservoir, Northeastern British Columbia, *Geoscience BC Report 2012-1*, 87–96.

Chalmers, G. R. L., D. J. K. Ross, and R. M. Bustin (2012). Geological controls on matrix permeability of Devonian gas shales in the Horn River and Liard basins, northeastern British Columbia, Canada, *Int. J. Coal Geol.* **103,** 120–131.

Clarke, H., J. P. Verdon, T. Kettlety, A. F. Baird, and J.-M. Kendall (2019). Real time imaging, forecasting and management of human-induced seismicity at Preston New Road, Lancashire, England, *Seismol. Res. Lett.* **90,** 1902–1915.

Cui, X., and B. Nassichuk (2018). Permeability of the Montney Formation in the Western Canada sedimentary basin: Insights from different laboratory measurements, *Bull. Can. Petrol. Geol.* **66,** 394–424.

Dahm, T., D. Becker, M. Bischoff, S. Cesca, B. Dost, R. Fritschen, S. Hainzl, C. D. Klose, D. Kühn, S. Lasocki, *et al.* (2013). Recommendation for the discrimination of human-related and natural seismicity, *J. Seismol.* **17,** 197–202.

Dahm, T., S. Cesca, S. Hainzl, T. Braun, and F. Krüger (2015). Discrimination between induced, triggered, and natural earthquakes close to hydrocarbon reservoirs: A probabilistic approach based on the modeling of depletion-induced stress changes and seismological source parameters, *J. Geophys. Res.* **120,** 2491–2509.

Davis, S. D., and C. Frohlich (1993). Did (or will) fluid injection cause earthquakes? Criteria for a rational assessment, *Seismol. Res. Lett.* **64,** 207–224.

Davis, S. D., P. A. Nyffenegger, and C. Frohlich (1995). The 9 April 1993 earthquake in south-central Texas: Was it induced by fluid withdrawal? *Bull. Seismol. Soc. Am.* **85,** 1888–1895.

Eaton, D. W., and N. Igonin (2018). What controls the maximum magnitude of injection-induced earthquakes? *The Leading Edge* **37,** 135–140.

Eaton, D. W., and R. Schultz (2018). Increased likelihood of induced seismicity in highly overpressured shale formations, *Geophys. J. Int.* **214,** 751–757.

Eaton, D. W., N. Igonin, A. Poulin, R. Weir, H. Zhang, S. Pellegrino, and G. Rodriguez (2018). Induced seismicity characterization during hydraulic-fracture monitoring with a shallow-wellbore geophone array and broadband sensors, *Seismol. Res. Lett.* **89,** 1641–1651.

Eyre, T. S., D. W. Eaton, M. Zecevic, D. D'Amico, and D. Kolos (2019). Microseismicity reveals fault activation before M_W 4.1 hydraulic-fracturing induced earthquake, *Geophys. J. Int.* **218,** 534–546.

Farahbod, A. M., H. Kao, D. M. Walker, and J. F. Cassidy (2015). Investigation of regional seismicity before and after hydraulic fracturing in the Horn River basin, northeast British Columbia, *Can. J. Earth Sci.* **52,** 112–122.

Foulger, G. R., M. P. Wilson, J. G. Gluyas, B. R. Julian, and R. J. Davies (2018). Global review of human-induced earthquakes, *Earth Sci. Rev.* **178,** 438–514.

Friesen, O. J., S. E. Dashtgard, J. Miller, L. Schmitt, and C. Baldwin (2017). Permeability heterogeneity in bioturbated sediments and implications for waterflooding of tight-oil reservoirs, Cardium Formation, Pembina Field, Alberta, Canada, *Mar. Petrol. Geol.* **82,** 371–387.

Frohlich, C., H. DeShon, B. Stump, C. Hayward, M. Hornbach, and J. I. Walter (2016). A historical review of induced earthquakes in Texas, *Seismol. Res. Lett.* **87,** 1022–1038.

Ghanbari, A., S. M. Werner, L. Sadownyk, M. Gonzalez, and P. K. Pedersen (2019). Characterization and evaluation of deltaic sandstone reservoirs of the Dunvegan formation, Kaybob South, *Core Conf.*, May 2019, AER Core Research Centre.

Ghanizadeh, A., C. R. Clarkson, A. Vahedian, O. H. Ardakani, J. M. Wood, and H. Sanei (2018). Laboratory-based characterization of pore network and matrix permeability in the Montney Formation: Insights from methodology comparisons, *Bull. Can. Petrol. Geol.* **66,** 472–498.

Ghofrani, H., and G. M. Atkinson (2020). Activation rate of seismicity for hydraulic fracture wells in the Western Canada sedimentary basin, *Bull. Seismol. Soc. Am.* **110,** no. 5, 2252–2271.

Goebel, T. H. W., E. Hauksson, F. Aminzadeh, and J.-P. Ampuero (2015). An objective method for the assessment of fluid injection-induced seismicity and application to tectonically active regions in central California, *J. Geophys. Res.* **120,** 7013–032, doi: 10.1002/2015JB011895.

Hosseini, B. K., and D. W. Eaton (2018). Fluid flow and thermal modeling for tracking induced seismicity near the Graham disposal well, British Columbia (Canada), *SEG 88th Annual Conf.*, Anaheim, California, Expanded Abstracts, 4987–4991.

Kettlety, T., J. P. Verdon, M. Hampson, and L. Craddock (2020). The M_L 2.9 August 2019 earthquake in Lancashire, UK, induced by hydraulic fracturing during Preston new road PNR-2 operations, *Seismol. Res. Lett.* **92,** no. 1, 151–169, doi: 10.1785/0220200187.

Kettlety, T., J. P. Verdon, M. Werner, and J.-M. Kendall (2020). Stress transfer from opening hydraulic fractures controls the distribution of induced seismicity, *J. Geophys. Res.* **125,** e2019JB018794, doi: 10.1029/2019JB018794.

Kettlety, T., J. P. Verdon, M. J. Werner, J.-M. Kendall, and J. Budge (2019). Investigating the role of elastostatic stress transfer during hydraulic fracturing-induced fault activation, *Geophys. J. Int.* **217,** 1200–1216.

McGarr, A. (2014). Maximum magnitude earthquakes induced by fluid injection, *J. Geophys. Res.* **119,** 1008–1019.

Mossop, G. D., and I. Shetsen (1994). *Geological atlas of the Western Canada sedimentary basin*, Canadian Society of Petroleum Geologists and Alberta Research Council, available at https://ags.aer.ca/reports/atlas-of-the-western-canada-sedimentary-basin.html (last accessed September 2021).

Mustanen, D., J. Fianu, and J. Pucknell (2017). Account of hydraulically fractured onshore wells in the UK and seismicity associated with these wells, *J. Petrol. Sci. Eng.* **158,** 202–221.

National Research Council (2013). *Induced Seismicity Potential in Energy Technologies*, The National Academies Press, Washington, D.C., 300 pp.

Oprsal, I., and L. Eisner (2014). Cross-correlation - an objective tool to indicate induced seismicity, *Geophys. J. Int.* **196,** 1536–1543, doi: 10.1093/gji/ggt501.

Passarelli, L., F. Maccaferri, E. Rivalta, T. Dahm, and E. A. Boku (2013). A probabilistic approach for the classification of earthquakes as 'triggered' or 'not triggered', *J. Seismol.* **17,** 165–187.

Pawley, S., R. Schultz, T. Playter, H. Corlett, T. Shipman, S. Lyster, and T. Hauck (2018). The geological susceptibility of induced earthquakes in the Duvernay play, *Geophys. Res. Lett.* **45,** 1786–1793.

Peña Castro, A. F., M. P. Roth, A. Verdecchia, J. Onwuemeka, Y. Liu, R. M. Harrington, Y. Zhang, and H. Kao (2020). Stress chatter via fluid flow and fault slip in a hydraulic fracturing induced earthquake sequence in the Montney formation, British Columbia, *Geophys. Res. Lett.* **47,** e2020GL087254, doi: 10.1029/2020GL087254.

Riazi, N., D. Eaton, and A. Aklilu (2020). Novel methods for characterizing induced seismicity in the Montney formation, British Colombia, Canada, *82nd EAGE Annual Conf. Expanded Abstracts*, Th_E106_03.

Ross, G. M., and D. W. Eaton (1999). Basement reactivation in the Alberta basin: Observational constraints and mechanical rationale, *Bull. Can. Petrol. Geol.* **47,** 391–411.

Roth, M. P., A. Verdecchia, R. M. Harrington, and Y. Liu (2020). High-resolution imaging of hydraulic fracturing-induced earthquake clusters in the Dawson-Septimus area, northeast British Columbia, Canada, *Seismol. Res. Lett.* **91,** 2744–2756.

Schoenball, M., N. C. Davatzes, and J. M. G. Glen (2015). Differentiating induced and natural seismicity using space-time-magnitude statistics applied to the Coso Geothermal field, *Geophys. Res. Lett.* **42,** 6221–6228.

Schultz, R., and R. Wang (2020). Newly emerging cases of hydraulic fracturing induced seismicity in the Duvernay East shale basin, *Tectonophysics* **779,** 228393, doi: 10.1016/j.tecto.2020.228393.

Schultz, R., G. Atkinson, D. W. Eaton, Y. J. Gu, and H. Kao (2018). Hydraulic fracturing volume is associated with induced earthquake productivity in the Duvernay play, *Science* **359,** 304–308.

Schultz, R., V. Stern, and Y. J. Gu (2014). An investigation of seismicity clustered near the Cordel Field, west central Alberta, and its relation to a nearby disposal well, *J. Geophys. Res.* **119,** 3410–3423.

Schultz, R., V. Stern, Y. J. Gu, and D. Eaton (2015). Detection threshold and location resolution of the Alberta Geological Survey earthquake catalogue, *Seismol. Res. Lett.* **86,** 385–397.

Shapiro, S. A., C. Dinske, and C. Langenbruch (2010). Seismogenic index and magnitude probability of earthquakes induced during reservoir fluid stimulations, *The Leading Edge* **29,** 304–309.

Skoumal, R. J., M. R. Brudzinski, and B. S. Currie (2018). Proximity of preCambrian basement affects the likelihood of induced seismicity in the Appalachian, Illinois, and Williston basins, central and eastern United States, *Geosphere* **14,** 1365–1379.

van der Elst, N. J., M. T. Page, D. A. Weiser, T. H. W. Goebel, and S. M. Hosseini (2016). Induced earthquake magnitudes are as large as (statistically) expected, *J. Geophys. Res.* **121,** no. 6, 4575–4590.

Verdon, J. P., and J. J. Bommer (2021). Green, yellow, red, or out of the blue? An assessment of traffic light schemes to mitigate the impact of hydraulic fracturing-induced seismicity, *J. Seismol.* **25,** 301–326.

Verdon, J. P., and J. Budge (2018). Examining the capability of statistical models to mitigate induced seismicity during hydraulic fracturing of shale gas reservoirs, *Bull. Seismol. Soc. Am.* **108,** 690–701.

Verdon, J. P., B. J. Baptie, and J. J. Bommer (2019). An improved framework for discriminating seismicity induced by industrial activities from natural earthquakes, *Seismol. Res. Lett.* **90,** 1592–1611.

Verdon, J. P., N. Igonin, J.-M. Kendall, and D. W. Eaton (2019). Fault reactivation via pre-existing fracture networks during hydraulic fracturing, society of earthquake and civil engineering dynamics conference, Greenwich London, *Conf. Proc. 7.4.*

Wetmiller, R. J. (1986). Earthquakes near Rocky Mountain House, Alberta, and their relationship to gas production facilities, *Can. J. Earth Sci.* **23,** 172–181.

Yassin, M. R., M. Begum, and H. Dehghanpour (2017). Organic shale wettability and its relationship to other petrophysical properties: A Duvernay case study, *Int. J. Coal Geol.* **169,** 74–91.

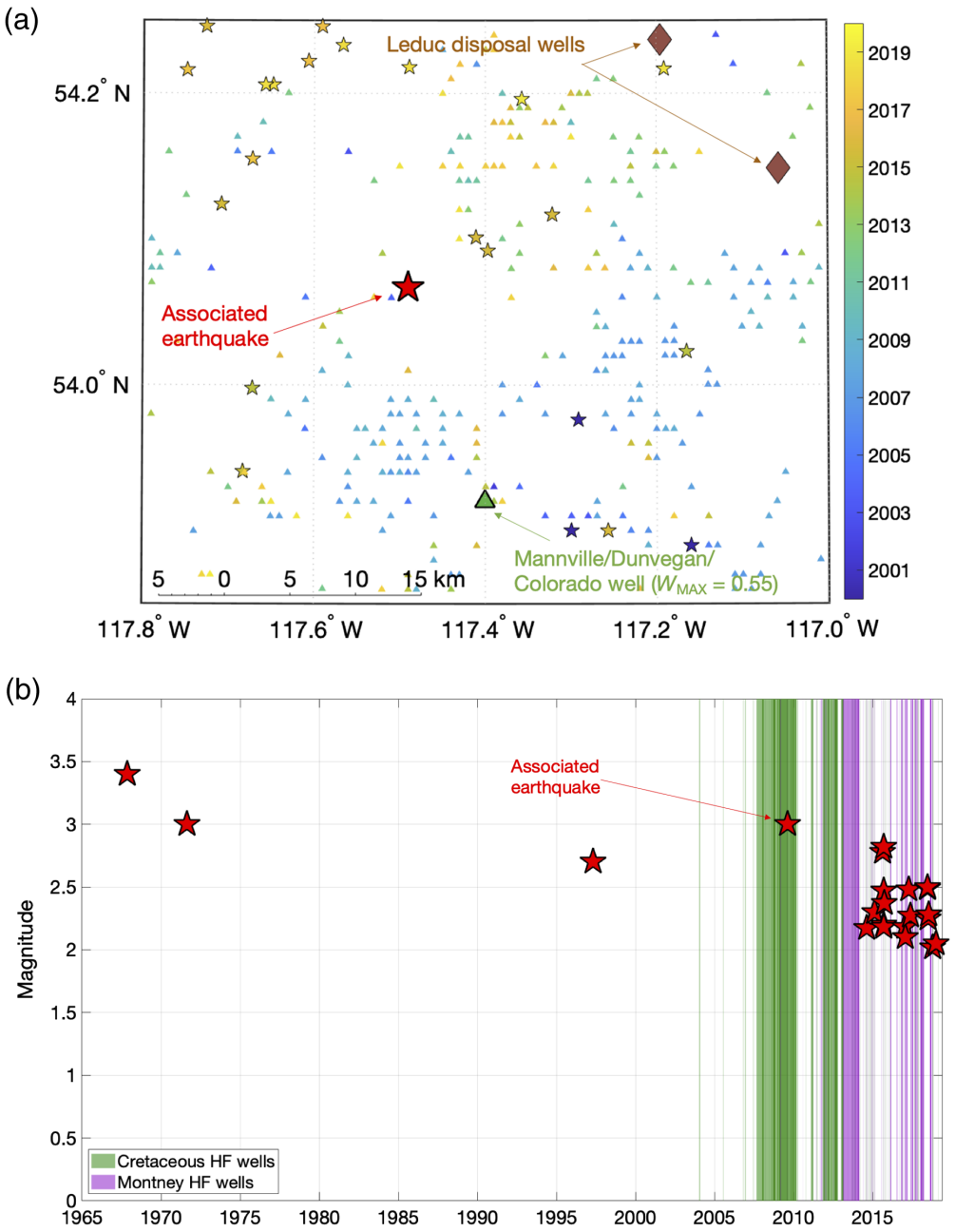

Figure A1. (a) Map and (b) timeline showing the event that occurred on 10 August 2009 near to Berland River that was linked by the Ghofrani and Atkinson (2020, hereafter, GA20) method with hydraulic fracturing (HF) in 5 collocated Mannville, Colorado, and Dunvegan wells (light green triangle). Other HF wells are shown (triangles), colored by the year in which HF took place. Two nearby high-volume injection wells are also highlighted, which target the Leduc formation. Stars show all **M** ≥ 2 earthquakes colored by their occurrence date—the event linked to the Mannville wells is marked by a red star. In (b), we show a timeline of earthquakes in this area (stars), with green (Cretaceous wells) and purple (Montney wells) shading showing dates when HF took place in the area. The color version of this figure is available only in the electronic edition.

APPENDIX
Case-by-case evaluation of Table 1 events

Berland River: 10 August 2009 M 3.0. A single event near to Berland River, to the south of Fox Creek, is linked by the Ghofrani and Atkinson (2020, hereafter, GA20) method with five collocated wells that target Mannville (Wilrich, 100/07-18-057-23W5/03; Gething, 100/07-18-057-23W5/02; Notikewin, 100/07-18-057-23W5/04), Colorado (100/07-18-057-23W5/06), and Dunvegan (100/07-18-057-23W5/05) formations.

Figure A1 shows a map of this event, and its relationship to adjacent oil and gas activities. The Mannville, Colorado, and Dunvegan wells are 17.4 km from the event and were stimulated by <300 m^3 of fluid each, between 4 August 2009 and 5 August 2009, five days before the event occurred. The largest *W*-value for these wells is 0.55. Worldwide, we are not aware of any cases of hydraulic fracturing-induced seismicity (HF-IS) being generated from injection of such small

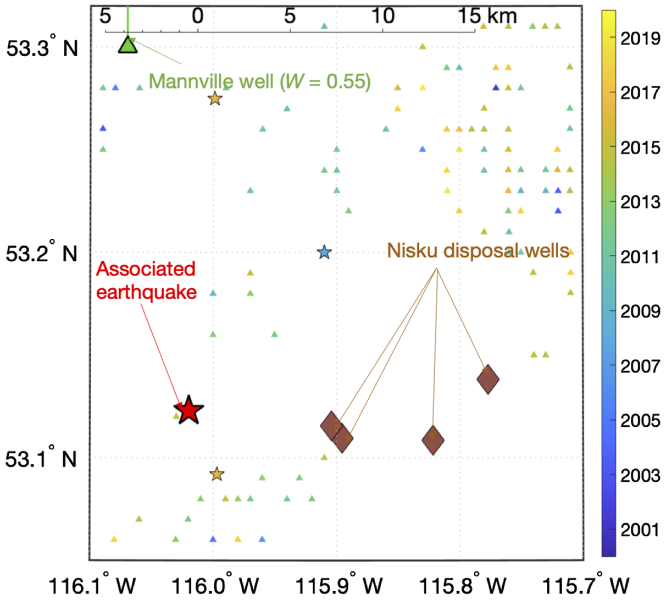

Figure A2. Map showing the event that occurred on 8 October 2010 near to Wolf Lake that was linked by the GA20 method with HF in a Mannville well (light green triangle with lines showing the well tracks in the subsurface). Four high-volume disposal wells targeting the Nisku formation (Devonian) are also marked by brown diamonds. Other stimulated wells (triangles) are also shown, colored by the year in which stimulation took place. Stars show **M** ≥ 2 earthquakes colored by their occurrence date—the event associated with the Mannville well is marked by a red star. The color version of this figure is available only in the electronic edition.

volumes of fluid. Given the very low volumes involved with these stimulations—2 orders of magnitude lower than the volumes typically associated with stimulation of the Duvernay and Montney, for example—any perturbation that they could cause would be limited to very close to the well. A location uncertainty that is significantly larger than that estimated by Schultz *et al.* (2015), and larger even than the 10 km location uncertainty adopted by GA20, would be required to collocate this event the Mannville, Colorado, and Dunvegan wells.

There are two high-volume injection wells that could present a more plausible potential cause for this event than the stimulated wells, given that these disposal wells have injected 3.5 orders of magnitude more fluid. These wells target the Devonian Leduc formation. However, because this is a single, isolated event, and that three events of similar magnitude have been observed in this area between 1960 and 2000, prior to the onset of hydraulic fracturing (HF) activities, it is more likely that this is a natural event. A large number of stimulated wells are present in the area. None of the other 500 Cretaceous wells in the area, most of which were stimulated between 2004 and 2012, are linked to any earthquakes. We note that a burst of seismicity begins in late 2014, which appears to correspond with the onset of HF in the underlying Montney formation.

Given the low volumes of fluid used to stimulate the identified wells, and the distances between the identified wells and the event, it is implausible that the 2009 event was triggered by activities in the wells to which the GA20 method has linked it.

Wolf Lake: 8 October 2010 M 3.2. This earthquake is located to the northwest of the Brazeau Reservoir. It was linked by the GA20 method to a well in the Mannville formation, with $W = 0.55$. Figure A2 shows a map of this event and its relationship to adjacent oil and gas activities.

The Mannville well (100/13-13-050-15W5/00) was stimulated on 5 October 2010, three days before the event. However, this well is 20.0 km from the event location. Event location uncertainties far higher than those estimated by Schultz *et al.* (2015), and those adopted by GA20, would be required to collocate this event with the identified Mannville well. The event is too far from the well for HF, using a volume of ~600 m^3 (the volume injected by this well), to be considered to be a plausible cause.

There are four high-volume water disposal wells in the area, the largest of which has injected over 2 million m^3 since 1990. These wells target the Devonian Nisku formation. It is possible that this event has a natural origin, and it is also possible that these disposal wells may have caused the identified event, especially because three other earthquakes have occurred in the vicinity of these disposal wells while they have been active. In contrast, any link with the identified Mannville well is clearly spurious, and it is again apparent that the association of the 8 October 2010 event with this well by the GA20 method is not plausible.

Fox Creek Duvernay: 15 January 2015 M 3.3. This earthquake is located in the Fox Creek region, where seismicity has been induced by stimulation of the Duvernay formation (e.g., Bao and Eaton, 2016). A map and timeline of these events and nearby oil and gas activities is shown in Figure A3.

The event was linked by the GA20 method ($W = 0.55$) to HF in one Dunvegan well (100/05-13-062-26W5/00). This well injected approximately 3000 m^3 of fluid, taking one day to complete, on 11 January 2015, four days before the occurrence of the associated event. However, the Dunvegan well is located over 19 km from the event, and so a very large location error would be required to collocate this event with the associated Dunvegan well.

This event has a much stronger link to a Duvernay well ($W = 0.85$) that was active at the time (100/15-15-062-23W5/02). The Duvernay well injected approximately 26, 000 m^3 and was active from 11 to 20 January 2015. The identified event is part of a cluster of **M** <3 events that occurred during stimulation of the Duvernay well. The identified event is located approximately 4 km from the toe of the Duvernay well, but given a reasonable

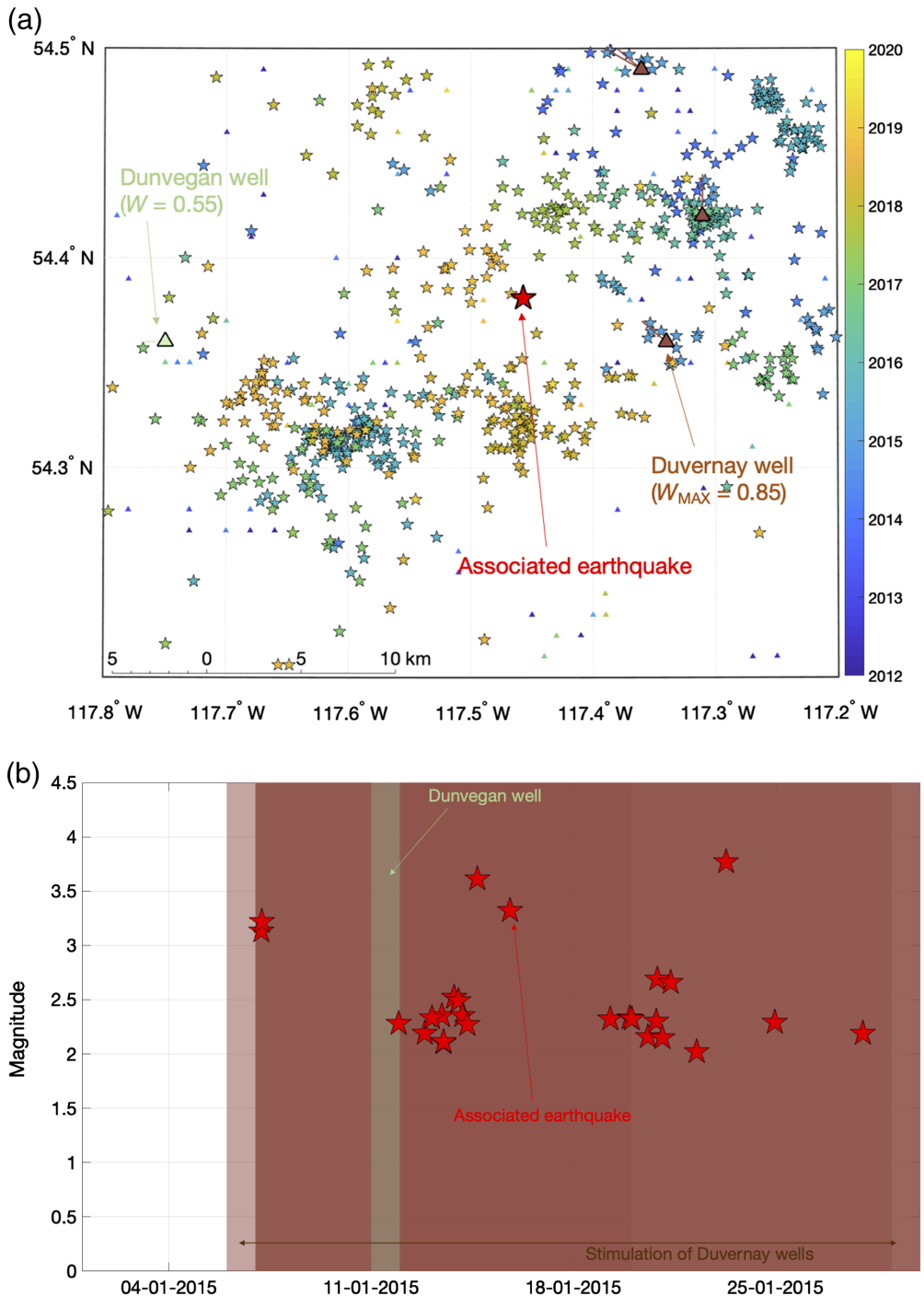

Figure A3. (a) Map and (b) timeline showing the earthquake that occurred during January 2015 that was associated by the GA20 method with HF in a Dunvegan well. In (a), the location of the Dunvegan well is shown by the light green triangle (and lines showing the well track in the subsurface), and the locations of several Duvernay wells that were also active at this time are shown as brown triangles. Other stimulated wells in the area are shown as triangles colored by the date of stimulation. The identified earthquake is shown as a red star, and all other $\mathbf{M} \geq 2$ earthquakes are shown as stars colored by occurrence date. In (b), we show the days in which HF took place in the Dunvegan (light green) and Duvernay (brown) wells, and the occurrence dates of nearby earthquakes. The color version of this figure is available only in the electronic edition.

location uncertainty of 3 km (based on Schultz *et al.*, 2015), the event could be within 1 km of the well.

We note that in table A1 of GA20, the Reference ID notes for this case identify this as one of the earthquakes studied by Bao and Eaton (2016), who explicitly linked this event and other clusters of seismicity in the area to HF of the Duvernay. It is clear that this event has been induced by stimulation of the Duvernay, and that any links to the Dunvegan well are not plausible.

Fox Creek Duvernay: 16 January 2017 M 3.0. Much like the previous example, this earthquake is located in the Fox Creek region, where hydraulic fracturing-induced seismicity (HF-IS) caused by stimulation of the Duvernay formation is extensively documented. This event was linked by the GA20 method (W = 0.36) to HF in a Dunvegan well (100/04-13-062-26W5/00). This well injected approximately 4000 m^3 of fluid, taking one day to complete, on 5 January 2017 (10 days before the occurrence of the identified event). This well is located over 10 km from the event location. Figure A4 shows a map and timeline of this case.

Much like the previous case, this event has a much stronger link (W = 1.0) to four Duvernay wells that were also active at the time (100/05-25-061-25W5/00, 100/11-25-061-25W5/00, 100/10-25-061-25W5/00, 100/06-25-061-25W5/00). These Duvernay wells all injected approximately 40, 000 m^3, and began operations on 5 January 2017, and were still undergoing

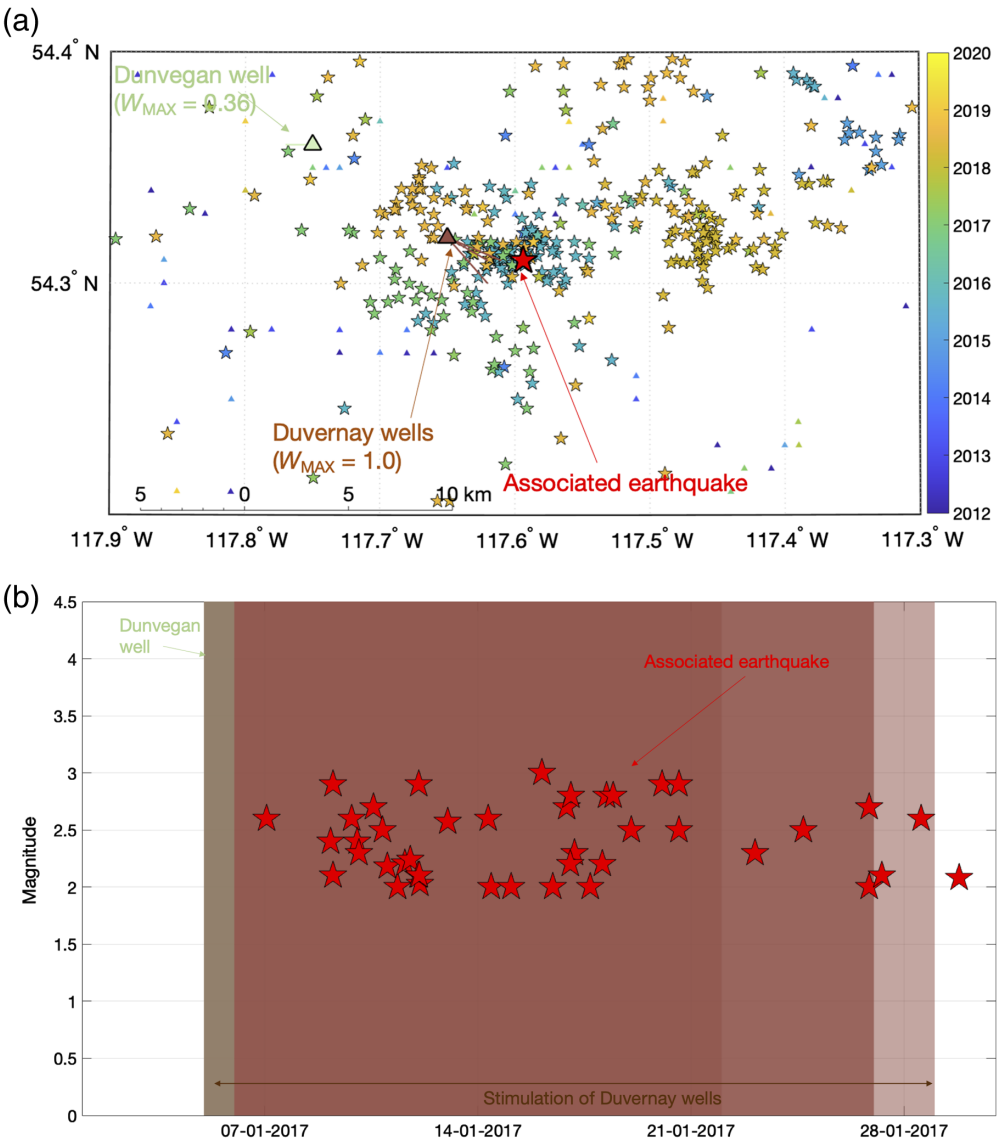

Figure A4. (a) Map and (b) timeline showing the earthquake in January 2017 that was linked by the GA20 method to HF in a Dunvegan well. In (a), the location of the Dunvegan well is shown by the light green triangle (and line showing the well track in the subsurface). Four Duvernay wells were also active at this time, shown by the brown triangle and lines. Other HF wells present in the area are also shown, colored by the date of stimulation. All $\mathbf{M} \geq 2$ earthquakes are shown, colored by their occurrence date—the event linked to the Dunvegan well is marked by a red star. In (b), we show the days in which stimulation took place in the Dunvegan (green) and Duvernay (brown) wells, and the occurrence dates of the nearby earthquakes. The color version of this figure is available only in the electronic edition.

stimulation when the identified event occurred. The event location is collocated with the subsurface tracks of the Duvernay wells and is part of a sequence of $\mathbf{M} < 3.0$ events that occurred around these Duvernay wells, which began at the same time that the Duvernay wells became active. As such, the link between these events and the Duvernay wells is clear and obvious, and it is equally clear that the association produced by the GA20 method between this event and the Dunvegan wells is not plausible.

Manuscript received 2 November 2020
Published online 19 October 2021